International Journal of Medical Microbiology 309 (2019) 151329

Contents lists available at ScienceDirect

International Journal of Medical Microbiology

journal homepage: www.elsevier.com/locate/ijmm

Consequences of dosing and timing on the antibacterial effects of ADEP antibiotics

Christian Mayer, Peter Sass*[,1], Heike Brötz-Oesterhelt*[,1]

Interfaculty Institute for Microbiology and Infection Medicine, Department for Microbial Bioactive Compounds, University of Tuebingen, Auf der Morgenstelle 28, 72076 Tuebingen, Germany

ARTICLE INFO

Keywords:
Antibiotic acyldepsipeptides
Caseinolytic protease
Staphylococcus aureus
MRSA
Bacillus subtilis

ABSTRACT

Antibiotic acyldepsipeptides (ADEPs) exert potent antibacterial activity in rodent models of bacterial infection and exceptional efficacy against persister cells of methicillin-resistant *Staphylococcus aureus* (MRSA). The mechanism of ADEP action is unusual in that the antibiotic releases the destructive capacity of over-activated ClpP, the proteolytic core of the bacterial Clp protease. The essential bacterial cell division protein FtsZ had emerged in a previous study as a preferred protein substrate of ADEP-activated ClpP but it is definitely not the only cellular substrate.

In the current study, we set out to follow the morphological changes that lead to ADEP-mediated bacterial death in *S. aureus* and *Bacillus subtilis,* differentiating between antibacterial effects at low and high ADEP concentrations. Here, fluorescence and time-lapse microscopy data show that cells adopt a characteristic phenotype of cell division inhibition at ADEP levels close to the MIC, but retain the capacity to form viable daughter cells for a substantial period of time when transferred to ADEP-free growth medium. After extended exposure to low ADEP concentrations, nucleoids of *B. subtilis* started to disorganize and upon compound removal many cells failed to re-organize nucleoids, re-initiate cytokinesis and consequently died. Survival *versus* cell death of filamentous cells attempting recovery depended on the timing of completion of new septa in relation to the loss of cell envelope integrity. We show that the potential to recover after ADEP removal depends on the antibiotic concentration as well as the treatment duration. When exposed to ADEP at concentrations well above the MIC, biomass production ceased rapidly as did the potential to recover. In time-kill studies both long-time exposure to low ADEP levels as well as short-time exposure to high concentrations proved highly effective, while intermittent concentrations and time frames were not. We here provide new insights into the antimicrobial activity of ADEP antibiotics and the consequences of dosing and timing for bacterial physiology which should be considered in view of a potential therapeutic application of ADEPs.

1. Introduction

Antibacterial resistance has become a major public health issue regarding the therapy of common infectious diseases. Given the dramatic increase of multidrug-resistant human pathogens, new antimicrobial agents with novel modes of action and resistance breaking properties are of urgent need. Acyldepsipeptide antibiotics (ADEP) are structurally unrelated to antibiotics in therapeutic application and demonstrated prominent antibacterial potency against many Gram-positive species, including methicillin-resistant *S. aureus* (MRSA), vancomycin-resistant enterococci and penicillin-resistant *Streptococcus pneumoniae* (Brötz-Oesterhelt et al., 2005; Hinzen et al., 2006). Furthermore, in combination with rifampicin, ADEP killed persister cells and eradicated a deep-seated biofilm in a mouse model (Conlon et al., 2013). ADEP has a unique mechanism of action. While most antibiotics currently approved for therapy operate by targeting one of the major biosynthetic pathways, *i.e.* the synthesis of DNA, RNA, peptidoglycan and proteins, ADEP acts by binding to the serine peptidase ClpP, the proteolytic core component of the ATP-dependent caseinolytic protease (Clp) (Brötz-Oesterhelt et al., 2005; Malik and Brötz-Oesterhelt, 2017) and lead to its deregulation.

Clp protease fulfills crucial functions in bacterial cells as it is associated with protein quality control and homeostasis as well as the post-transcriptional regulation of virulence factors, morphological differentiation, and stress tolerance (Brötz-Oesterhelt and Sass, 2014; Bukau et al., 2006; Frees et al., 2004, 2014). Here, proteolytic activity of the

* Corresponding authors.
E-mail addresses: peter.sass@uni-tuebingen.de (P. Sass), heike.broetz-oesterhelt@uni-tuebingen.de (H. Brötz-Oesterhelt).
[1] These authors share senior authorship.

https://doi.org/10.1016/j.ijmm.2019.151329
Received 13 April 2019; Received in revised form 2 July 2019; Accepted 9 July 2019

core ClpP strictly depends on its interaction with partner Clp-ATPases (*i.e.* ClpC, ClpE, and ClpX in *Bacillus subtilis*), which unfold natural substrates by consuming ATP and insert the unfolded polypeptide chains into the degradation chamber of the barrel-shaped ClpP tetradecamer (Baker and Sauer, 2012; Kirstein et al., 2009b; Olivares et al., 2016).

ADEP-mediated deregulation of Clp protease is multifaceted. By binding to ClpP, ADEP displaces partner Clp-ATPases, thereby preventing the formation of a functional Clp protease complex and, consequently, all physiological functions of the Clp protease in the cellular context (Kirstein et al., 2009a). We have previously shown that such inhibition of the natural Clp functions leads to cell death of mycobacteria (Famulla et al., 2016). In addition, binding of ADEP to the ClpP core also induces a conformational change of ClpP which locks the tetradecamer in an extended, active conformation (Gersch et al., 2015). This conformational change triggers an enlargement of the apical and distal entrance pores of ClpP, which now allow the entry of non-native polypeptide and protein substrates to the proteolytic chamber, thereby conferring independent proteolytic activity to the otherwise dormant core ClpP (Kirstein et al., 2009a; Lee et al., 2010; Li et al., 2010).

In addition to the different effects on its direct cellular target, ADEP also leads to distinct phenotypes of treated bacteria at low *versus* high antibiotic concentrations, thus implicating different consequences for bacterial physiology. At low inhibitory ADEP concentrations (approx. 2-3-fold the minimal inhibitory concentration, MIC), ADEP-treated *S. aureus* swells up to three times the size of a normal cell, and *B. subtilis* cells are characterized by a filamentous phenotype with cells reaching up to 100-fold the length of untreated cells. Under these conditions, biosynthetic capacity of treated cells is still remarkable and the syntheses of DNA, RNA, peptidoglycan and proteins proceed unaffected for several hours (Sass et al., 2011). The increase in cell volume can be explained by the fact that ADEP activates ClpP to degrade the essential cell division protein FtsZ in *S. aureus* and *B. subtilis* (Sass and Brötz-Oesterhelt, 2013; Sass et al., 2011). Such untimely degradation of FtsZ leads to the inhibition of divisome formation and cell division and, ultimately, to bacterial cell death (Sass et al., 2011). However, using higher ADEP concentrations (*e.g.* > 10x MIC), the effect on treated cells changes dramatically. Here, ADEP leads to rapid cessation of biomass production with a concomitant drop in colony forming units (CFU) (Sass et al., 2011), clearly indicating detrimental effects of ADEP treatment that go beyond inhibition of cell division. ADEP-activated ClpP was also shown to degrade nascent peptide chains emerging from the ribosome (Kirstein et al., 2009a) and hundreds of non-native peptide fragments had emerged in treated bacteria after extended exposure to elevated ADEP concentrations (Conlon et al., 2013).

In the current study, we set out to further characterize these different antibacterial effects in relation to the antibiotic concentration and investigated the associated morphological changes in a time-resolved manner and on the single cell level. It emerged that low *versus* high ADEP concentrations result in different effects, both leading to bacterial cell death, but on a different time scale and by a different manner. Importantly, intermittent concentrations and exposure times allowed treated cells to recover growth when transferred to ADEP-free conditions.

2. Material and methods

2.1. Bacterial strains and growth conditions

All bacterial strains, plasmids and primers used in this study are listed in Table 1. Bacterial strains were grown in lysogeny broth (LB) at 37 °C. For preparation of solid media, agar-agar (Roth) was added to a final concentration of 1.5%. When necessary, the growth medium was supplemented with the appropriate antibiotic using the following concentrations: spectinomycin, 100 µg/ml; chloramphenicol, 5 µg/ml (for *B. subtilis*); erythromycin, 2 µg/ml (for *S. aureus*); and ampicillin, 100 µg/ml (for *Escherichia coli*). Xylose and IPTG were used as inducers at concentrations of 0.1 - 0.2% or 0.1 mM, respectively. *E. coli* XL1-blue (Agilent Technologies), *E. coli* DH5α (Invitrogen), and *E. coli* DC10B (Monk et al., 2012) were used as cloning hosts for plasmid construction.

2.2. Construction of plasmids and bacterial strains

For the construction of plasmid pACM01, *ftsZ* was amplified from chromosomal DNA of *B. subtilis* strain 168 with primers oCM13 and oCM14. The resulting PCR fragment was then inserted by a Gibson isothermal assembly reaction into the integrative vector pAPNC (Jahn et al., 2015; Morimoto et al., 2002) that had previously been digested with *Eco*RI and *Bam*HI. Transformation of *B. subtilis* strain 168 with pACM01 resulted in strain CM01. Plasmid pHJCM01 was derived from pHJS105 (Jahn et al., 2015). For construction, the plasmid was PCR amplified using oligonucleotides oCM01 and oCM02 to introduce a glycine-serine-rich linker between the protein of interest and monomeric superfolder green fluorescent protein (sfGFP) (Pedelacq et al., 2006). Plasmid pJCM02 was generated by ligation of the PCR amplified coding sequence of *noc*, digested with *Eco*RI and *Bam*HI, into plasmid pJCM01, which had previously been digested with the same restriction enzymes. *noc* was amplified using primers oCM05 and oCM06. The resulting plasmid was integrated into the *amyE* locus of strain CM01 to give strain CM02. Standard techniques were used for molecular cloning (Anagnostopoulos and Spizizen, 1961; Gibson et al., 2009; Sambrook et al., 1989).

2.3. OD- and kill curve

For OD- and kill curve experiments, *S. aureus* HG001 was incubated overnight at 37 °C. LB medium was inoculated with an overnight culture to 10^5 CFU/ml. ADEP2 at concentrations of 1 µg/ml, 8 µg/ml and 48 µg/ml was added to the flasks (t = 0) and the cultures were further incubated at 37 °C. An untreated culture served as a control. After 10 min (for the 48 µg/ml sample) and 1 h (for the 8 µg/ml sample) cells were harvested and washed twice with pre-warmed LB medium. Cells were then resuspended in fresh pre-warmed LB medium containing no antibiotic. Samples for OD measurement and CFU determination were collected every 2 h. For this, a 1:10 dilution series in sterile 0.9% NaCl of each sample per time point was prepared and 10 µl of each dilution was plated onto LB-agar plates. After overnight incubation at 37 °C, colonies grown were counted and CFUs calculated with the following formula:

$$\text{CFU/ ml} = \text{number of counted colonies} * \text{dilution} * 1/(\text{volume [ml]})$$

2.4. ADEP treatment and recovery

For microscopic analyses, *B. subtilis* overnight cultures were grown in LB medium (supplemented with appropriate antibiotics), inoculated into fresh LB medium (supplemented with inducers for the expression of fluorophore-labeled proteins) and further grown at 37 °C to an optical density of 600 nm (OD_{600}) of 0.1 at which ADEP2 was added at concentrations indicated in the respective figures. Samples were taken at distinct time points as indicated and analyzed by phase contrast and fluorescence microscopy. For recovery experiments, cells treated with ADEP2 were harvested in a table top centrifuge at 1500 g and inoculated into fresh, pre-warmed ADEP-free LB medium supplemented with the appropriate inducers for the expression of fluorophore-labeled proteins. Images were taken at indicated time points after transfer of the bacteria into ADEP-free medium.

2.5. Microscopic imaging and microfluidics

For microscopy experiments, samples were mounted on microscopy slides coated with a thin layer of 1% agarose in water or growth medium to immobilize cells. For time course studies, cells were grown to an OD_{600} of 0.1. Preparation of microscopy samples was performed as previously described (de Jong et al., 2011d), with the only difference

Table 1
Strains, plasmids and primers used in this study.

Strains	Genotype/ Properties/ Nucleotide sequence (5'-3')	Induction used	Reference/ Source
B. subtilis			
168	*trpC2*	–	Laboratory Stock
CM01	*trpC2 (aprE::cat Pspac-mcherry-ftsZ)*	0.1 mM IPTG	This study
CM02	*trpC2 (aprE::cat Pspac-mcherry-ftsZ)*	0.1 mM IPTG	This study
	(amyE::spc Pxyl-sfgfp-noc)	0.1% xylose	
S. aureus			
RNpPBP2-31	RN4220 derivative with *gfp-pbp2* fusion	0.2% xylose	(Pinho and Errington, 2005)
RN1HG001	$rbsU^+$, $tcaR^-$	–	(Herbert et al., 2010)
E. coli			
XL1-blue	*recA1 endA1 gyrA96 thi-1 hsdR17 supE44 relA1 lac[F′ proAB lacI^{q}ZΔM15* Tn*10* (Tet^r)*]*		Agilent Technologies
DH5α	*F– Φ80lacZΔM15 Δ(lacZYA-argF) U169 recA1 endA1 hsdR17 (rK–, mK +) phoA supE44 λ– thi-1 gyrA96 relA1*		Invitrogen
DC10B	*dam$^+$ Δdcm ΔhsdRMS endA1 recA1*		(Monk et al., 2012)
Plasmids			
pAPNC	*aprE Pspac-mCherry-MCS, bla, cat*		(Jahn et al., 2015; Morimoto et al., 2002)
pACM01	*aprE Pspac-mCherry-ftsZ, bla cat*		This study
pHJS105	*amyE Pxyl-msfgfp-MCS, spc bla*		(Jahn et al., 2015)
pHJCM01	*amyE Pxyl-msfgfp-linker-MCS- spc bla*		This study
pHJCM02	*amyE Pxyl-msfgfp-linker-noc, spc bla*		This study
Primers			
oCM01[1]	*GAGCTCTACAAAGGCTCAGGAAGCGGCAAAATGTCCAGAC*		This study
oCM02[1]	*GTCTGGACATTTTGCCGCTTCCTGAGCCTTTGTAGAGCTC*		This study
oCM03	*CGCGGATCCACAAGCATTCATTCTCTCGTTTC*		This study
oCM04	*CCGGAATTCCTATTTTGGTATGCGAATCGTTAATTG*		This study
oCM13	*CAAATCAGGAAGCGGCTCAGGATCCTTGGAGTTCGAAACAAACATAG*		This study
oCM14	*TGCGCTTGGGCTAACGCCCGTTAGCCGCGTTTATTACG*		This study

[1] oCM01 and oCM02 are 5` phosphorylated.

that half-concentrated LB ($LB_{50\%}$) was used. Where appropriate, ADEP2 was added at a concentration of 0.125 µg/ml (2-fold MIC) to the agarose. For recovery experiments, we conducted time-lapse experiments using the CellASIC ONIX microfluidic platform using microfluidic plates for bacterial cells (B04A-03-5PK). The microfluidic platform had been coupled to a Nikon Eclipse Ti-E microscope. After 2 or 6 h of ADEP treatment, cultures with an OD_{600} of 0.01 were loaded with 10 psi pressure from valve six and eight for 10 s, after which it was rinsed with a pressure of 1 psi for 30 s. During the microfluidic experiment, the media flow rate was maintained at 2 psi at a temperature of 37 °C for the growth of *B. subtilis*. DNA and membranes were visualized, when needed, by staining the cells with 4′,6-diamidino-1-phenylindole (DAPI; 1 µg/mL; Sigma-Aldrich) and FM5-95 (10 µg/ml; Molecular Probes), respectively. Fluorescence microscopy was carried out using a Nikon Eclipse Ti microscope equipped with an ORCA-Flash 4.0 L T camera (Hamamatsu) and a Cage Incubator (Okolab) or by employing the Zeiss LSM800 super-resolution, confocal microscope equipped with Airyscan technology. For confocal imaging, the fluorophores GFP and FM5-95 were excited at 488 nm and 506 nm, respectively. The window for detecting emission wavelengths were set to 485–520 nm for GFP and 650–700 nm for FM5-95. Images were acquired using NIS Elements Advanced Research (Nikon) or ZEN software packages (Zeiss). For analyzing time course studies, images were taken every 7.5 min or 15 min. Further analyses and processing of images were performed in NIS Elements, ZEN and Fiji software (Schindelin et al., 2012).

3. Results

3.1. ADEP concentration and exposure time are critical for bacterial killing

To characterize the two distinct phenotypes observed with ADEP-treated cells, we first addressed the specific relation between bacterial killing and the applied antibiotic concentration with respect to the exposure time. To this end, we conducted OD- and time-kill experiments and applied distinct exposure regimes that reflected the two extremes 1) long-term exposure at a low concentration *versus* 2) very short exposure at a very high concentration as well as 3) an intermittent situation with exposure to an intermediate concentration for an intermediate time frame. Following these exposure set-ups, cells were monitored for their capacity to recover by following the optical density OD_{600} and by determining colony forming units. In this experiment, we used *S. aureus* as a relevant human pathogen and deliberately decided to use the derivative ADEP2 to ensure comparability with our previous studies on the molecular and cellular effects of ADEP.

In the field of pharmacokinetics, the area under the concentration curve (AUC) is the integral in a plot of drug concentration in blood plasma *versus* time. Of course, in our study we worked *in vitro*, in culture broth instead of plasma and we applied and removed ADEP batch-wise rather than simulating a proper pharmacokinetic curve. However, we took particular care to apply such antibiotic concentrations and incubation times which resulted in all three cases in the equivalent of an equal AUC (proxy here: concentration multiplied by time exposed) value of 8 (Fig. 1A). When *S. aureus* cultures were treated with 1 µg/ml ADEP2 (2x MIC) for a period of 8 h (simulating long-term exposure at a low concentration), CFUs dropped from the initial inoculum and the culture did not increase in OD over time (Fig. 1B and C, blue lines). Also, when we applied the other extreme, 48 µg/ml ADEP2 (96x MIC) for 10 min, simulating a very short exposure at a very high concentration, growth inhibition was strong with a concurrent decline in CFU (Fig. 1B and C, red lines). In contrast, when cells were exposed to 8 µg/ml ADEP2 (16x MIC) for 1 h (simulating the intermittent situation with respect to time and concentration), we observed an increase in OD and CFU after 4 to 6 h, clearly distinguishing this situation as less effective (Fig. 1B and C, green lines). The data show that the applied ADEP concentration in relation to the exposure time is critical for bacterial killing and, rather unusually, both extremes, low-level / long-term as well as high-level / short-term are highly efficient.

3.2. ADEP-treated S. aureus can re-initiate cell division when returned to non-inhibiting conditions

Since the capacity of bacterial cells to recover from treatment with a given antibiotic is an important information to be considered in putative future application regimes, we next set out to further investigate

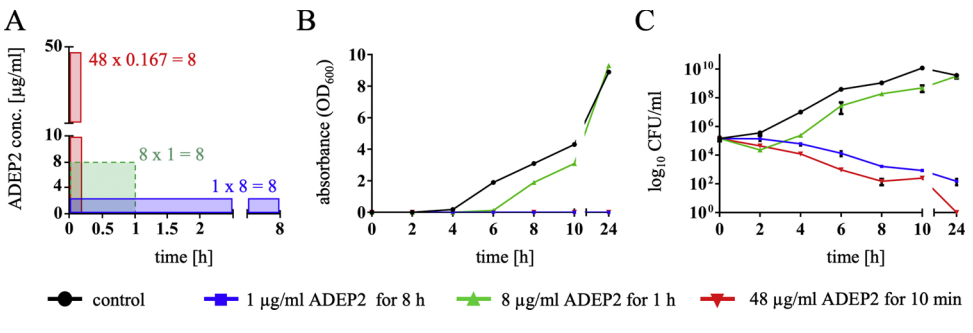

Fig. 1. Antimicrobial activity of ADEP against *S. aureus* is concentration- and time dependent. (A) Schematic representation of the different exposure regimes used in the growth and time-kill experiment. At time zero three different concentrations of ADEP were added in parallel to aliquots of the same culture and exposed to the antibiotic for the indicated different periods of time. Concentrations multiplied by the time exposed were used as a proxy of the AUC and were set to 8 in all three cases. (B) Growth curve of *S. aureus* HG001 in LB medium recorded as OD_{600} and starting from an inoculum of 10^5 CFU/ml. (C) Corresponding time-kill experiment recorded by determining the number of colony forming units. For CFU determination, bacteria were plated on ADEP-free agar, thus allowing recovery of still viable cells. Error bars indicate standard deviations of three independent biological replicates.

the recovery process on the single-cell level by fluorescence microscopy. In order to monitor cell division in this process we employed a *S. aureus* strain expressing GFP-tagged penicillin-binding protein 2 (GFP-PBP2) (Table 1) and treated it with either low or high inhibitory concentrations of ADEP2. PBP2 is a bifunctional protein, comprising a transpeptidase and transglycosylase domain, which is involved in the synthesis of septal peptidoglycan. PBP2 was shown to localize to the division site of *S. aureus* and this localization is dependent on FtsZ-ring formation (Pinho and Errington, 2003, 2005). Previous results had shown that GFP-PBP2 delocalizes from the septal area of *S. aureus* upon treatment with ADEP and that this delocalization is a direct consequence of the degradation of FtsZ by ADEP-ClpP (Sass et al., 2011). Corroborating this, in our current study GFP-PBP2 delocalized from the septal area of *S. aureus* upon treatment with low the ADEP2 concentration (1 µg/ml, 2x MIC) for 6 h, as indicated by its shifted localization to the periphery of the cell compared to untreated control cells (Fig. 2A, i and ii). When we then transferred treated *S. aureus* cells into ADEP-free medium, we indeed observed newly dividing cells after additional 2 h and 4 h recovery time, as indicated by emerging visible septa, stained by the lipophilic membrane dye FM5-95, and GFP-PBP2 localization at mid-cell (Fig. 2A, iii and iv). However, when we attempted to recover *S. aureus* cells that had been exposed to higher inhibitory concentrations of ADEP2 (8 µg/ml, 16x MIC) for 6 h, the examined cells did not regain septal localization of GFP-PBP2 (Fig. 2B). These data link the recovery of ADEP-treated cells to the re-initiation of bacterial cell division.

3.3. Recovery of filamentous *B. subtilis* cells depends on ADEP concentration and exposure time

Compared to *S. aureus*, the phenotype of rod-shaped *B. subtilis* cells is even more severe and involves strong filamentation of treated cells at antibiotic concentrations closely above the MIC (approx. 2x MIC), generating filaments that can reach cell lengths of more than 200 µm. Thus, we next studied whether such extreme filamentous cells show the same capacity to recover from ADEP treatment when returned to antibiotic-free conditions. To investigate this, we treated *B. subtilis* strain CM01 (Table 1), which expresses mCherry-FtsZ under the control of an IPTG-inducible promotor from the ectopic *aprE*-locus, with 0.125 µg/ml ADEP2 (2x MIC) for 4 h. Native *ftsZ* was retained in its original locus. As expected, cells formed long filaments at this antibiotic concentration (Fig. 3A; Movie S1). To test whether this filamentation phenotype is reversible, we transferred the filaments into ADEP-free growth medium. And indeed, we noticed that the transferred cells were capable of re-initiating the formation of FtsZ-rings after 2 h followed by successful daughter cell separation as indicated by the appearance of normally sized cells after 4 h (Fig. 3B). Noteworthy, newly formed FtsZ-rings appeared all over the filamentous cell with no obvious preference regarding its location. There was no preference for the mid-cell position. This result indicates that low inhibitory concentrations of ADEP indeed result in filamentous *B. subtilis* cells that, in principle, remain fully viable for a certain period of time (at least 4 h under the condition applied here). Even after this period cells are able to recover from ADEP treatment and are capable of returning to a normal cell cycle and cytokinesis.

As the phenotypes of ADEP-treated *B. subtilis* cells also differ in response to the ADEP concentration applied, we next tested whether either increased ADEP concentrations (> 10x MIC) or prolonged treatment duration at lower concentrations affect the ability of the cells for recovery. Although our previous data had indicated that increased ADEP concentrations result in the inhibition of growth and a concomitant drop in CFU (Sass et al., 2011), the effects had never been investigated on the level of single cells, neither was there information on the recovery potential. To address these questions, we incubated mCherry-FtsZ expressing *B. subtilis* cells with low (0.125 µg/ml, 2x MIC) or high (0.75 µg/ml, > 10x MIC) inhibitory ADEP concentrations. When *B. subtilis* was treated with ADEP over a short time period of 2 h (Fig. 4A, i), the low inhibitory ADEP concentration allowed re-initiation of FtsZ-ring formation approx. 2 h after the removal of ADEP and showed cells of normal size after 4 h (~100% cells were able to recover; n > 100) (Fig. 4A, ii and iii; Movie S2). When the concentration was increased to > 10x MIC of ADEP, the cells showed a different phenotype and were shorter (Fig. 4A, ii) compared to cells treated at low ADEP level. After 2 h of treatment at > 10x MIC, only approx. 50% of monitored cells were able to recover and recovery was clearly delayed. Cells were defined as “unable to recover” when no visible Z-rings were detected or when cells were lysed (results from three independent experiments, n > 50) (Fig. 4A, v and vi; Movie S3). When the exposure time was extended to 6 h, recovery was already delayed at low inhibitory ADEP concentrations (Fig. 4B, ii and iii; Movie S4) and only 40% of the cells were able to re-initiate Z-ring formation (results from three independent experiments, n > 100). At > 10x MIC and an exposure time of 6 h, cells were characterized by an uneven cell structure and a lack of the typical filamentation phenotype, indicating severe cellular damage. Recovery potential was completely lost (all monitored cells were unable to recover Z-ring formation; n > 50) (Fig. 4B, iv-vi; Movie S5). Thus, our data show that, depending on the applied ADEP concentration as well as the duration of antibiotic treatment, ADEP exerts both reversible and irreversible damage to the bacterial cell.

3.4. ADEP-induced depletion of FtsZ results in *B. subtilis* cells containing highly mis-segregated nucleoids

Since only 40% of *B. subtilis* cells were able to recover growth when treated at low inhibitory concentrations for the longer exposure time of 6 h, further effects have to prevent recovery in addition to sole inhibition of FtsZ-ring formation. Prolonged depletion of FtsZ in *B. subtilis*, and consequently blockage of cell division, had previously been associated with inhibition of DNA replication (Arjes et al., 2014). To study whether ADEP treatment has a similar effect on the morphology of nucleoids, we next investigated the integrity of nucleoids using the nucleic acid stain DAPI in *B. subtilis* cells which had been depleted of

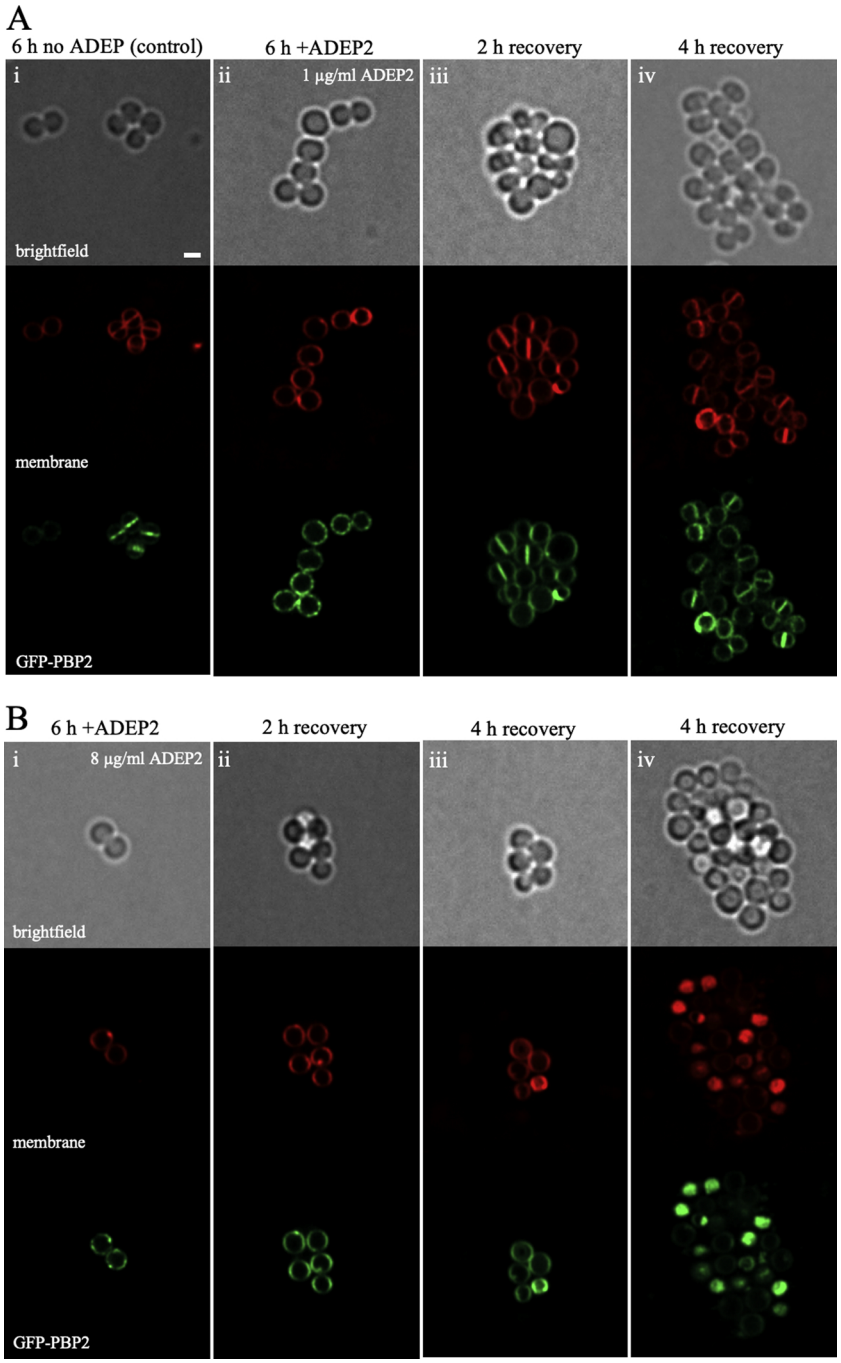

Fig. 2. Re-initiation of divisome formation in *S. aureus* after compound withdrawal. (A,B) Localization of GFP-PBP2 in ADEP-treated *S. aureus* strain RNpPBP2-31 and subsequent recovery from antibiotic treatment. (A) Cells were grown in xylose-supplemented LB medium (0.2% final concentration) at 37 °C to an OD_{600} of 0.1 (10^8 CFU/ml) which was then supplemented with ADEP2 (1 µg/ml ADEP2; 2x MIC). After 6 h of treatment the compound was removed and cells were allowed to recover. Samples were drawn immediately before ADEP removal (ii) as well as after 2 h (iii) and 4 h (iv) of recovery time. Compared to untreated control cells (i) the low inhibitory ADEP concentration (ii) led to a delocalization of PBP2 in *S. aureus*, which could be reversed even after 6 h of ADEP treatment as indicated by the re-localization of GFP-PBP2 after to 2–4 h of growth in ADEP-free medium (iii and iv). (B) In contrast, 6 h of incubation at a high inhibitory ADEP concentration (i; 8 µg/ml ADEP2; 16x MIC) prevented re-initiation of divisome formation after compound removal (ii, iii, iv), and cells started to show additional defects as demonstrated by abnormal membrane staining and clustered GFP-PBP2 localization (iv), indicating severe cell damage and/or cell death even during recovery conditions. Images are representative of at least three independent biological replicates. Scale bars represent 1 µm for all images.

FtsZ (and potentially further proteins) by incubation with low inhibitory ADEP concentrations (0.125 µg/ml, 2x MIC) for 6 h. In such filamentous cells deprived of FtsZ by extended ADEP exposure, we consistently observed a clearly dispersed DAPI signal, indicating severe mis-segregation of nucleoids (Fig. 5A). In clear contrast, cells that had been treated for only 2 h showed normal nucleoid morphology with well-segregated chromosomes (Fig. 5D). When we then transferred long-term exposed *B. subtilis* with dispersed nucleoids into ADEP-free medium, the individual filaments showed a heterogeneous behavior. While approx. 40% ($n > 100$) of the filamentous cells re-initiated Z-ring formation after being returned to non-inhibiting conditions (Fig. 5B), others maintained a diffuse nucleoid distribution, potentially accompanied by DNA degradation, and these cells failed to re-initiate cell division (Fig. 5C). Interestingly, when applying high inhibitory ADEP concentrations we already observed detrimental effects on nucleoids after 2 h of treatment, supporting the idea of additional damage to the cells under these conditions.

3.5. Survival of recovering cells depends on cell envelope integrity

In principle, our data show that bacterial cells may remain viable over a longer period of time at lower concentrations of ADEP2, however, also these cells eventually die when ADEP exposure proceeds. Thus, we next studied the reasons that lead to bacterial cell death under these conditions. Since an ADEP-treated, filamentous *B. subtilis* cell may be regarded as a consortium of single cells lacking cell separation by division septa, we hypothesized that defects in the cell envelope may be a predominant cause of cell death under these ADEP-treatment conditions, as a defect in one cell segment directly and severely affects the entire filamentous cell. To test this hypothesis, we treated a *B. subtilis*

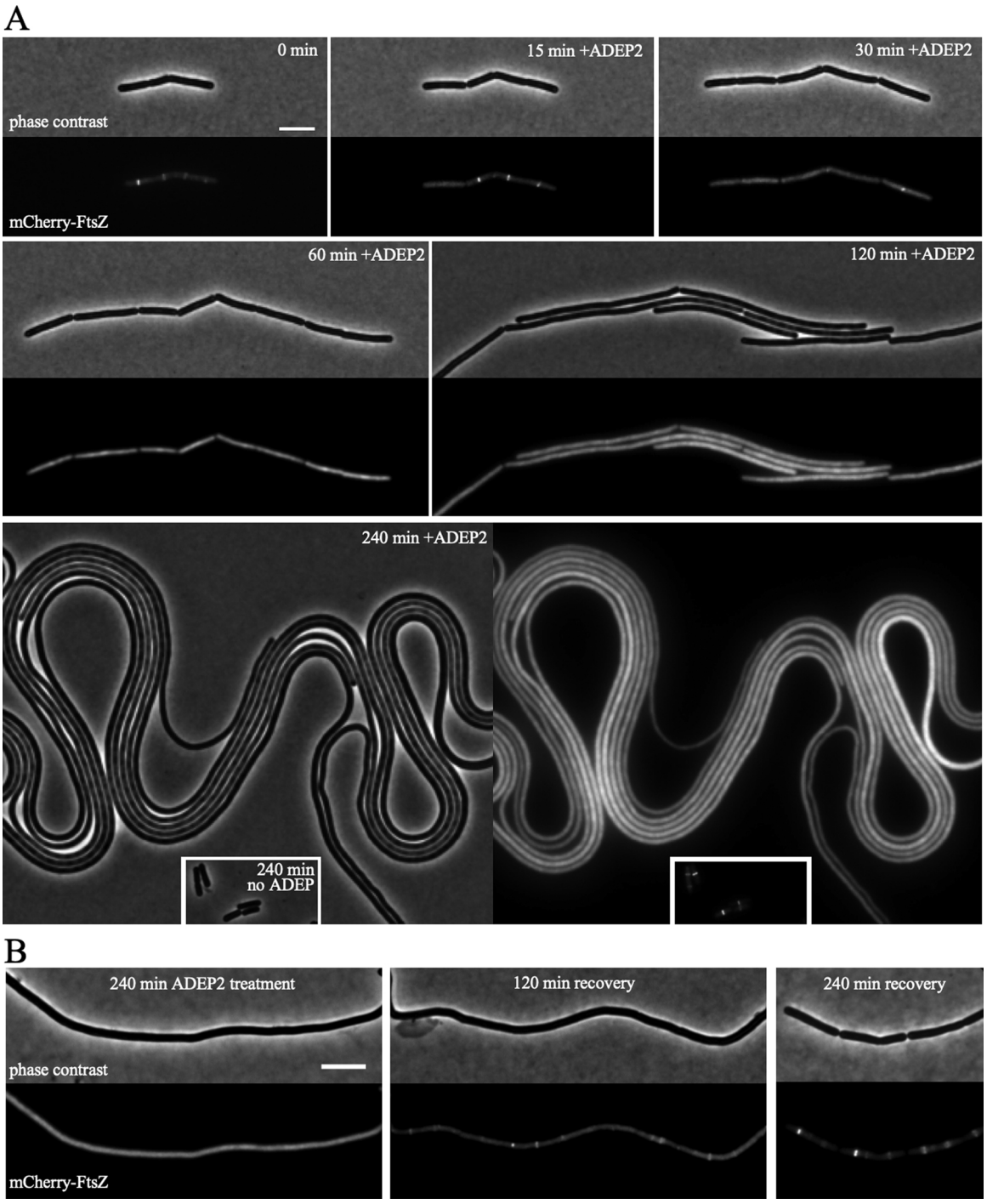

Fig. 3. ADEP-treated *B. subtilis* cells recover FtsZ-ring formation after transfer to ADEP-free growth medium. (A) Time-lapse study of *B. subtilis* strain CM01 (*aprE::cat-Pspac-mcherry-ftsZ*) during 4 h of continuous treatment at low ADEP level and localization of mCherry-FtsZ. Strain CM01 was grown in LB medium in the presence of 0.1 mM IPTG at 37 °C to an OD_{600} of 0.1 (5×10^7 CFU/ml). Then cells were transferred to an agarose-coated microscopy slide supplemented with 0.125 µg/ml ADEP2 (2x MIC) and 0.1 mM IPTG (for the expression of mCherry-FtsZ). Phase contrast and fluorescence images were taken every 7.5 min for a time period of 240 min. Images are representative of at least three independent biological replicates. Scale bar, 5 µm. (B) Localization of mCherry-FtsZ of *B. subtilis* strain CM01 during recovery from ADEP treatment. Strain CM01 was first treated with ADEP (0.125 µg/ml ADEP2; 2x MIC) for 4 h and was then transferred to ADEP-free growth medium. Images were acquired after 2 h and 4 h of recovery and are representative of at least three independent biological replicates. Scale bar, 5 µm.

strain expressing mCherry-FtsZ and GFP-Noc with 0.125 µg/ml ADEP2 (2x MIC) for 5 h and then followed the recovery of treated cells in ADEP-free medium *via* time-lapse microscopy. Noc is a DNA-binding protein involved in nucleoid occlusion, a regulatory system in *B. subtilis* responsible for preventing division over nucleoids. Noc binds to specific DNA sequences (Noc-binding sites) distributed over wide regions of the chromosome (Wu et al., 2009; Adams et al., 2015), and thus can be used to visualize correct nucleoid segregation in time-course experiments. The filamentous cells shown in Fig. 6 and Movie S6 still depicted normal nucleoid morphology when ADEP was withdrawn and FtsZ-rings re-appeared approx. 15–30 min after removal of ADEP. However, before successful cell division was achieved, FtsZ-rings disappeared again and the organization of nucleoids was lost (Fig. 6, *45 min*), which was the result of a cell envelope lesion as indicated in phase contrast

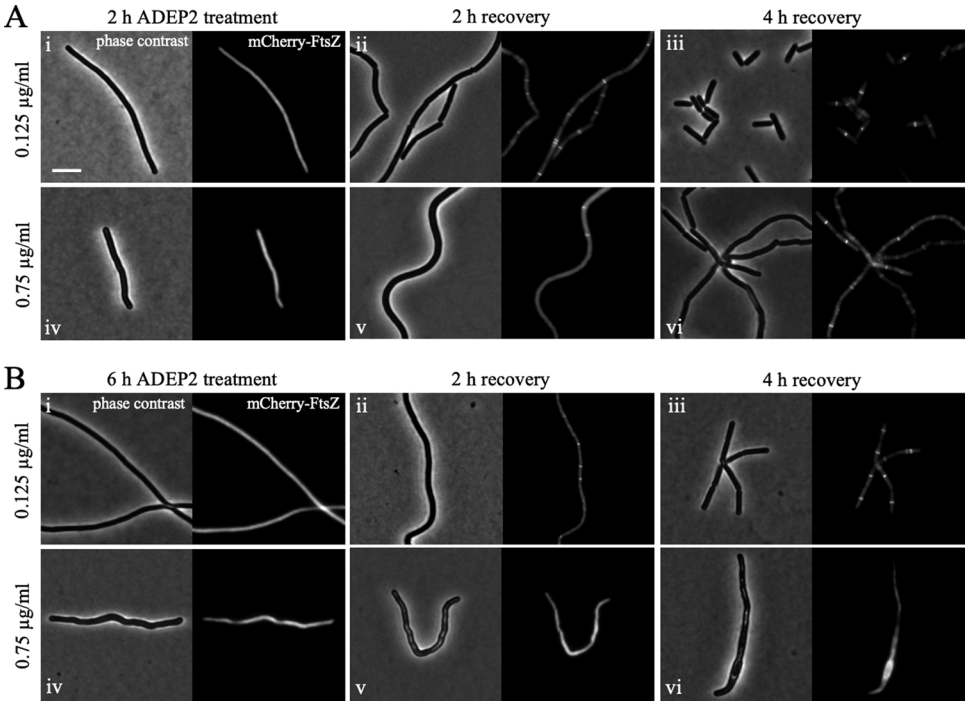

Fig. 4. Re-initiation of FtsZ-ring formation in *B. subtilis* is delayed at increased ADEP concentration and after prolonged treatment duration. (A) Localization of mCherry-FtsZ during recovery of *B. subtilis* strain CM01 (*aprE::cat-Pspac-mcherry-ftsZ*) from short-term ADEP treatment. Strain CM01 was treated at an OD_{600} of 0.1 with either a low inhibitory (0.125 µg/ml ADEP2; 2x MIC, upper panel) or a high inhibitory (0.75 µg/ml ADEP2; > 10x MIC, lower panel) ADEP concentration for 2 h before cells were transferred to ADEP-free conditions and monitored for a further 2–4 h. Images are representative of at least three independent biological replicates. Scale bar, 5 µm. (B) Localization of mCherry-FtsZ during recovery of *B. subtilis* strain CM01 (*aprE::cat-Pspac-mcherry-ftsZ*) after prolonged ADEP treatment. Strain CM01 was treated with either a low inhibitory (0.125 µg/ml ADEP2; 2x MIC, upper panel) or a high inhibitory (0.75 µg/ml ADEP2; > 10x MIC, lower panel) ADEP concentration for a prolonged period of 6 h before transfer of the cells to ADEP-free conditions for 2–4 h. Images are representative of at least three independent biological replicates. Scale bar, 5 µm.

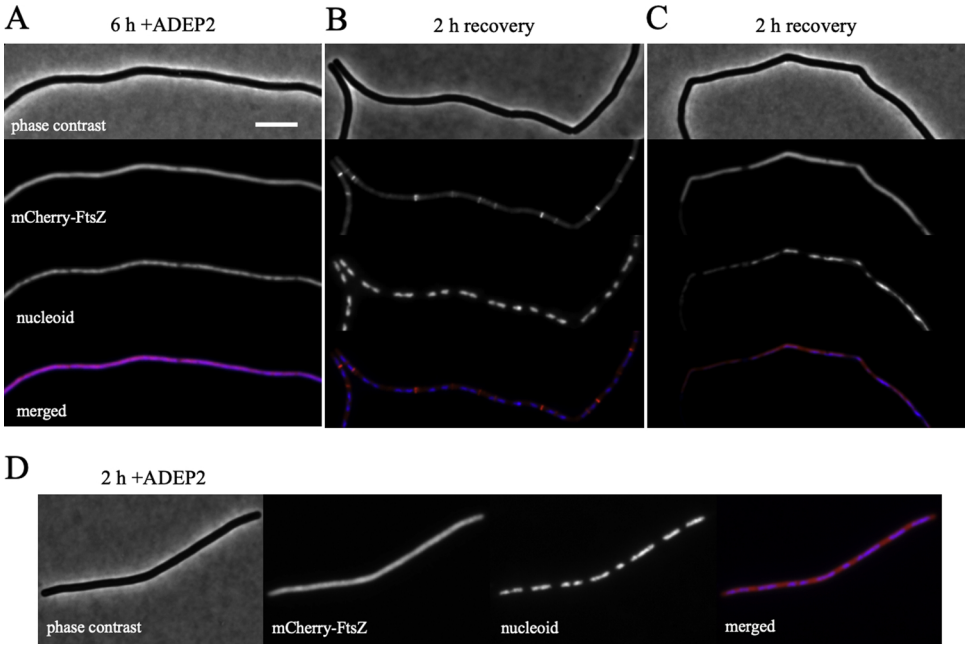

Fig. 5. Prolonged ADEP treatment results in aberrant nucleoid morphology. (A,B,C) Localization of mCherry-FtsZ and nucleoids (stained with DAPI) during ADEP treatment and recovery. (A) *B. subtilis* strain CM01 (*aprE::cat Pspac-mcherry-ftsZ*) was grown in IPTG-supplemented LB medium at 37 °C to an OD_{600} of 0.1 after which ADEP2 (0.125 µg/ml, 2x MIC) was added to the culture. Phase contrast and fluorescence images were taken after 6 h of ADEP treatment. (B,C) Long-term exposed filamentous *B. subtilis* cells with dispersed nucleoids showed a heterogeneous behavior after being transferred into ADEP-free medium (2 h recovery). Approx. 40% (n > 100) of the filamentous cells re-initiated Z-ring formation (B), whereas others maintained a diffuse nucleoid distribution and failed to re-initiate cell division (C). (D) *B. subtilis* cells show normal nucleoid morphology after short-term ADEP treatment for 2 h. All images are representative of at least three independent biological replicates. Scale bar, 5 µm.

micrographs (Fig. 6, *45 - 120 min*), causing death of the entire filamentous cell. This observation explains why a substantial amount of cells is unable to recover from long-term ADEP treatment at low inhibitory concentrations.

As shown above, filamentous cells may also survive when transferred to ADEP-free medium, as indicated in Fig. 7. In the filament shown here this happened after approx. 60–120 min of recovery. However, a smaller terminal part of the filamentous cell survived and eventually divided into viable daughter cells (Fig. 7, *120–480 min*; Movie S7). In this case, the filamentous cell had been able to complete a new septum in time before cell envelope lesions occurred. Thus, our results show that under this particular condition of low inhibitory ADEP concentrations close to the MIC, *B. subtilis* cells may remain viable for several hours, and can potentially recover, even from a phenotype of extreme filamentation, if ADEP is withdrawn. However, recovery strongly depends on the accomplishment of successful cell division events before cell envelope integrity gets lost. Timing is highly critical, as a single cell envelope lesion affects the entire filamentous consortium.

4. Discussion

The mechanism of ADEP action is multifaceted and so are the resulting antibacterial effects that can be observed at different conditions of treatment. In the current study, we analyzed the different phenotypes observed with ADEP-treated *S. aureus* and *B. subtilis* cells, two Gram-positive bacteria with different morphologies and different organization of cell division. Phenotypes of FtsZ depletion have previously been

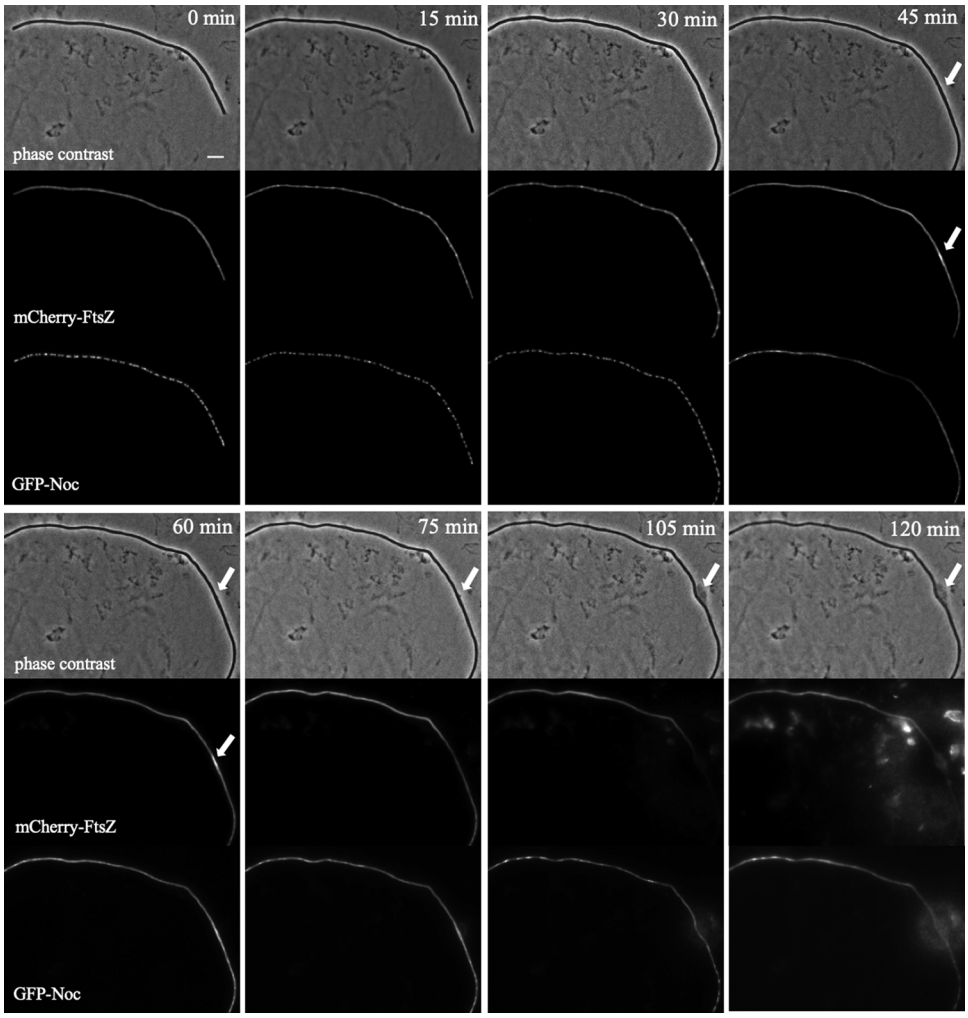

Fig. 6. Time-course of non-recovering *B. subtilis* cells after prolonged ADEP treatment. Localization of mCherry-FtsZ and GFP-Noc in *B. subtilis* strain CM02 (*aprE::cat Pspac-mcherry-FtsZ, amyE::spc Pxyl-gfp-noc*). Strain CM02 was treated with a low inhibitory concentration of ADEP2 (0.125 µg/ml, 2x MIC) for 5 h and was then transferred to an agarose-coated microscopy slide containing ADEP-free growth medium supplemented with 0.1 mM IPTG and 0.1% xylose and the fate of the cells was followed for further 2 h. Here, cell envelope integrity of the filamentous cell was lost after 75 min of recovery (indicated by arrows), which was fatal for the entire filamentous cell. All images are representative examples of at least three independent biological replicates. Scale bar, 5 µm.

studied in both organisms using cells that were depleted of FtsZ by genetic down-regulation (Beall and Lutkenhaus, 1991; Surdova et al., 2013) or by using inhibitors that directly interact with FtsZ, such as the benzamide antibiotic PC190723 which stimulates FtsZ over-polymerization (Adams et al., 2011; Andreu et al., 2010; Haydon et al., 2008; Stokes et al., 2013). However, ADEP-associated depletion of FtsZ differs from these situations, as FtsZ protein is rapidly degraded in treated cells and other targets of ADEP-activated ClpP may be involved as well. Therefore, we here investigated the ADEP phenotypes in more detail and addressed the antibacterial effects of ADEP concentration in relation to the exposure time. Our results clearly show that, in principle, *S. aureus* cells remain viable when short exposure times are chosen in combination with low inhibitory antibiotic concentrations, and cells are able to recover growth and form a colony when ADEP is removed. Under these conditions, also filamentous *B. subtilis* cells remained viable for a longer period of time as they showed a remarkable potential for the re-initiation of FtsZ-rings, cell division and finally daughter cell separation after being transferred into ADEP-free growth medium.

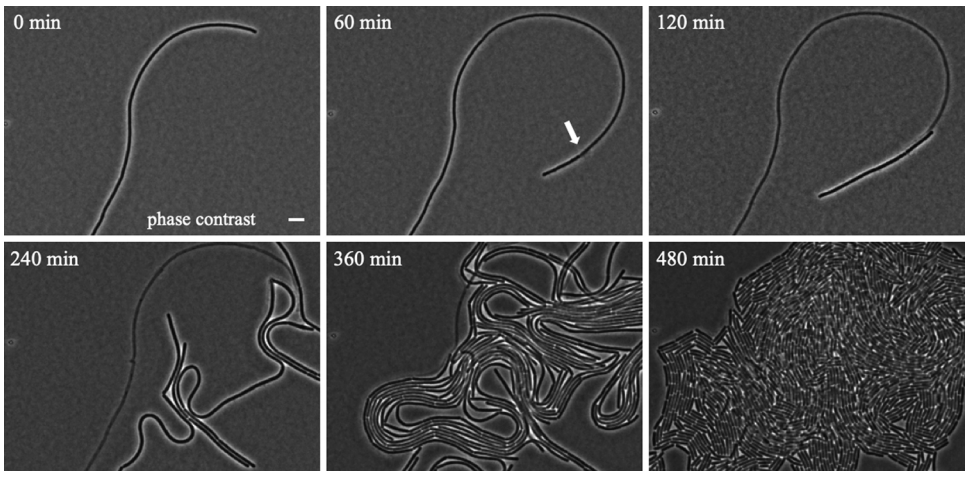

Fig. 7. Time-course of surviving *B. subtilis* cells after prolonged ADEP treatment. *B. subtilis* strain 168 wild type was treated with a low inhibitory concentration of ADEP2 (0.125 µg/ml, 2x MIC) for 5 h and was then transferred to an agarose-coated microscopy slide containing ADEP-free growth medium for recovery (0–480 min). Here, formation of a new septum occurred in time, before the structural integrity of the cell envelope was lost (indicated by an arrow), which allowed for the survival of the separated part of the filamentous cell that gave rise to new a colony of viable daughter cells. All images are representative examples of at least three independent biological replicates. Scale bar, 5 µm.

During recovery, newly formed FtsZ-rings re-appeared irregularly over the filament, however, exclusively in areas devoid of nucleoids and thus most probably guided by nucleoid occlusion (Cho et al., 2011; Wu and Errington, 2004; Wu et al., 2009). This is in agreement with previous observations made in *B. subtilis*, where visible FtsZ-rings in filaments depleted for FtsW were rather irregular spaced after re-induction of FtsW (Gamba et al., 2016). Importantly, successful recovery of *S. aureus* and *B. subtilis* was clearly dependent on the applied ADEP concentration as well as the duration of treatment.

When either the ADEP concentration or the duration of treatment were increased, re-initiation of FtsZ-ring formation was delayed followed by complete inhibition. *B. subtilis* exposed to elevated ADEP concentrations did not show a filamentation phenotype and rapid growth inhibition was accompanied by cell bulging and severe bending, which may be related to a depletion of cell envelope/ division proteins and proteins of the central dogma (*e.g.*, ribosomal proteins) (Kawai et al., 2009; Peters et al., 2016; Popham and Setlow, 1996), respectively. At higher ADEP concentrations and well in accordance with the broad destructive capacity of ADEP-activated ClpP, additional and non-reversible damage is afflicted to the cells as further proteins (in addition to FtsZ) are increasingly depleted (Conlon et al., 2013; Kirstein et al., 2009a).

Although reversible to some extent, bacteria are also killed at low inhibitory ADEP concentrations and the current study provides clues how this happens. We show that prolonged ADEP treatment of *B. subtilis* at low ADEP level eventually leads to an aberrant nucleoid morphology. This situation marks a kind of viability switch at which some cells are still capable of re-organizing nucleoids and survive, while other cells fail in chromosome re-organization and die. This nucleoid disorganization is in line with previous reports where bactericidal antibiotic treatment eventually led to chromosome condensation and DNA fragmentation (Dwyer et al., 2012). Also, in a study where *B. subtilis* with genetically down-regulated expression of *ftsZ* was investigated, cells also remained metabolically active, but after prolonged depletion of FtsZ, they were unable to initiate new rounds of either DNA replication or division when shifted to permissive conditions, thereby resembling our results observed at extended ADEP treatment duration (Arjes et al., 2014). In the same study, an extended block in cell division lead to growth arrest and entry into a permanent, quiescent state at the so-called *point of no return* (PONR). Transcriptional FtsZ knock-down cells which had passed the PONR, were unable to recover when shifted back to permissive conditions. This correlates with our finding that 60% of the cells treated with low inhibitory ADEP concentrations for the longer exposure time of 6 h were unable to recover and may thus have already passed the PONR. The cells studied by Arjes and colleagues already reached the PONR in approx. 4 h, which may be due to the different strain backgrounds or underlying principles of FtsZ depletion (genetic downregulation *versus* proteolysis by ADEP deregulated ClpP). In accordance with our findings, *E. coli* cells deprived of FtsZ have also been shown to contain an aberrant high number of unsegregated nucleoids, which may be due to a misplacement of FtsK, and cells displayed properly segregated nucleoids when FtsZ synthesis was restored (Sanchez-Gorostiaga et al., 2016). Both results from *E. coli* and *B. subtilis* indicate that a lack of FtsZ alone is sufficient to finally trigger an abnormal nucleoid morphology and cell death. Although transcriptional down-regulation of FtsZ and ADEP-mediated post-translational FtsZ proteolysis by ClpP represent two different mechanistic ways of depleting FtsZ, our current results show that low-level / long-term ADEP exposure results in a phenotype strongly reminiscent of FtsZ down-regulation. However, in our case it cannot be excluded that further degradation targets of ADEP-activated ClpP may further contribute to disorganization of nucleoids und bacterial killing under these conditions.

As we observed that some filamentous *B. subtilis* cells can remain viable at low inhibitory ADEP concentrations for several hours, while other filamentous cells already die earlier, we questioned how the bacteria are actually killed under these conditions. Time-resolved microscopy of ADEP-treated cells indicated that this is due to the filamentous habitus of the cells. In a filamentous cell, which may be considered as a consortium of multiple cells that are connected without interjacent division septa, defects of many vital cellular processes in one cellular segment can be compensated for by the remaining biosynthetic capacity of other cell segments, since, for example, metabolic products and proteins can diffuse unhindered throughout the cytosol as well as the membrane. However, what cannot be compensated for is cell envelope damage, as a single cell envelope lesion will inevitably result in cell death of the entire consortium. Thus, while being more robust to mutations affecting a variety of processes, the filament is not protected by the consortium against cell envelope defects. In this context, it is also noteworthy that cell envelope integrity was compromised in FtsZ-depleted *E. coli* cells (Sanchez-Gorostiaga et al., 2016), indicating that cells lacking FtsZ are particularly prone to cell envelope damage, thus, accelerating the frequency of lysis events. This is also true for *B. subtilis* cells with genetically downregulated FtsZ, since filamentous cells depleted of FtsZ were shown to be prone to lysis (Beall and Lutkenhaus, 1991; Surdova et al., 2013). Accordingly, we observed cell lysis in a large number of filaments in our study, during extended continuous exposure to ADEP as well as in the process of recovering from the antibiotic. However, FtsZ degradation may not be the only factor contributing to the lysis prone phenotype of ADEP treated cells. By abrogating the interaction of ClpP with cognate Clp-ATPases ADEP impairs the physiological functions of the Clp proteolytic complex, which controls multiple steps in cell wall metabolism including the amount of several autolysins and various cell wall synthesizing enzymes (Frees et al., 2014). During recovery, the fate of the bacterial cell to live or die seems to substantially depend on the speed of re-initiation of FtsZ-rings and successful septum completion in relation to the occurrence of the first cell envelope lesion.

In summary, we here provide novel insights into the antibacterial effects of ADEP antibiotics and show that ADEP, depending on antibiotic concentration and the duration of treatment, evokes distinct phenotypes, each eventually leading to bacterial cell death. Both long-time exposure to low ADEP levels as well as short-time exposure to high concentrations proved highly effective in killing the bacteria. However, our study also revealed the capacity of treated bacteria to recover cell growth and division when intermittent ADEP concentrations and exposure times are used. Thus, dosing and timing should be carefully considered regarding a potential application of ADEP antibiotics.

Author contributions

CM and PS conducted all experiments, analyzed data and prepared figures; CM, PS and HBO wrote the paper; CM, PS, and HBO designed research; PS and HBO obtained funding and directed research.

Acknowledgments

We gratefully thank L. Hamoen, M. Pinho, J. Errington, F. Götz and H. Strahl for the kind gift of strains and plasmids, and we acknowledge the technical support of S. Frank. We further thank A. Berscheid for critical discussions. The authors appreciate funding by the Deutsche Forschungsgemeinschaft (DFG, German Research Foundation)SFB766, TRR261.

Appendix A. Supplementary data

Supplementary material related to this article can be found, in the online version, at doi:https://doi.org/10.1016/j.ijmm.2019.151329.

References

Adams, D.W., Wu, L.J., Czaplewski, L.G., Errington, J., 2011. Multiple effects of benzamide antibiotics on FtsZ function. Mol.Microbiol. 80, 68–84.
Adams, D.W., Wu, L.J., Errington, J., 2015. Nucleoid occlusion protein Noc recruits DNA to the bacterial cell membrane. EMBO J. 34, 491–501.
Anagnostopoulos, C., Spizizen, J., 1961. Requirements for transformation of *Bacillus subtilis*. J. Bacteriol. 81, 741–746.

Andreu, J.M., Schaffner-Barbero, C., Huecas, S., Alonso, D., Lopez-Rodriguez, M.L., Ruiz-Avila, L.B., Nunez-Ramirez, R., Llorca, O., Martin-Galiano, A.J., 2010. The antibacterial cell division inhibitor PC190723 is an FtsZ polymer-stabilizing agent that induces filament assembly and condensation. J. Biol. Chem. 285, 14239–14246.
Arjes, H.A., Kriel, A., Sorto, N.A., Shaw, J.T., Wang, J.D., Levin, P.A., 2014. Failsafe mechanisms couple division and DNA replication in bacteria. Curr. Biol. CB 24, 2149–2155.
Baker, T.A., Sauer, R.T., 2012. ClpXP, an ATP-powered unfolding and protein-degradation machine. Biochim. Biophys. Acta 1823, 15–28.
Beall, B., Lutkenhaus, J., 1991. FtsZ in *Bacillus subtilis* is required for vegetative septation and for asymmetric septation during sporulation. Genes Dev. 5, 447–455.
Brötz-Oesterhelt, H., Beyer, D., Kroll, H.P., Endermann, R., Ladel, C., Schroeder, W., Hinzen, B., Raddatz, S., Paulsen, H., Henninger, K., Bandow, J.E., Sahl, H.G., Labischinski, H., 2005. Dysregulation of bacterial proteolytic machinery by a new class of antibiotics. Nat. Med. 11, 1082–1087.
Brötz-Oesterhelt, H., Sass, P., 2014. Bacterial caseinolytic proteases as novel targets for antibacterial treatment. Int. J. Med. Microbiol. 304, 23–30.
Bukau, B., Weissman, J., Horwich, A., 2006. Molecular chaperones and protein quality control. Cell 125, 443–451.
Cho, H., McManus, H.R., Dove, S.L., Bernhardt, T.G., 2011. Nucleoid occlusion factor SlmA is a DNA-activated FtsZ polymerization antagonist. Proc. Natl. Acad. Sci. U. S. A. 108, 3773–3778.
Conlon, B.P., Nakayasu, E.S., Fleck, L.E., LaFleur, M.D., Isabella, V.M., Coleman, K., Leonard, S.N., Smith, R.D., Adkins, J.N., Lewis, K., 2013. Activated ClpP kills persisters and eradicates a chronic biofilm infection. Nature 503, 365–370.
de Jong, I.G., Beilharz, K., Kuipers, O.P., Veening, J.W., 2011d. Live cell imaging of *Bacillus subtilis* and *Streptococcus pneumoniae* using automated time-lapse microscopy. J. Vis. Exp.
Dwyer, D.J., Camacho, D.M., Kohanski, M.A., Callura, J.M., Collins, J.J., 2012. Antibiotic-induced bacterial cell death exhibits physiological and biochemical hallmarks of apoptosis. Mol. Cell 46, 561–572.
Famulla, K., Sass, P., Malik, I., Akopian, T., Kandror, O., Alber, M., Hinzen, B., Ruebsamen-Schaeff, H., Kalscheuer, R., Goldberg, A.L., Brötz-Oesterhelt, H., 2016. Acyldepsipeptide antibiotics kill mycobacteria by preventing the physiological functions of the ClpP1P2 protease. Mol. Microbiol. 101 (2), 194–209.
Frees, D., Chastanet, A., Qazi, S., Sorensen, K., Hill, P., Msadek, T., Ingmer, H., 2004. Clp ATPases are required for stress tolerance, intracellular replication and biofilm formation in *Staphylococcus aureus*. Mol. Microbiol. 54, 1445–1462.
Frees, D., Gerth, U., Ingmer, H., 2014. Clp chaperones and proteases are central in stress survival, virulence and antibiotic resistance of *Staphylococcus aureus*. Int. J. Med. Microbiol. 304, 142–149.
Gamba, P., Hamoen, L.W., Daniel, R.A., 2016. Cooperative recuitment of FtsW to the division site of *Bacillus subtilis*. Front. Microbiol. 7, 1808.
Gersch, M., Famulla, K., Dahmen, M., Gobl, C., Malik, I., Richter, K., Korotkov, V.S., Sass, P., Ruebsamen-Schaeff, H., Madl, T., Brötz-Oesterhelt, H., Sieber, S.A., 2015. AAA+ chaperones and acyldepsipeptides activate the ClpP protease via conformational control. Nat. Commun. 6, 6320.
Gibson, D.G., Young, L., Chuang, R.Y., Venter, J.C., Hutchison 3rd, C.A., Smith, H.O., 2009. Enzymatic assembly of DNA molecules up to several hundred kilobases. Nat. Methods 6, 343–345.
Haydon, D.J., Stokes, N.R., Ure, R., Galbraith, G., Bennett, J.M., Brown, D.R., Baker, P.J., Barynin, V.V., Rice, D.W., Sedelnikova, S.E., Heal, J.R., Sheridan, J.M., Aiwale, S.T., Chauhan, P.K., Srivastava, A., Taneja, A., Collins, I., Errington, J., Czaplewski, L.G., 2008. An inhibitor of FtsZ with potent and selective anti-staphylococcal activity. Science 321, 1673–1675.
Herbert, S., Ziebandt, A.K., Ohlsen, K., Schäfer, T., Hecker, M., Albrecht, D., Novick, R., Götz, F., 2010. Repair of global regulators in *Staphylococcus aureus* 8325 and comparative analysis with other clinical isolates. Infect. Immun. 78, 2877–2889.
Hinzen, B., Raddatz, S., Paulsen, H., Lampe, T., Schumacher, A., Häbich, D., Hellwig, V., Benet-Buchholz, J., Endermann, R., Labischinski, H., Brötz-Oesterhelt, H., 2006. Medicinal chemistry optimization of acyldepsipeptides of the enopeptin class antibiotics. ChemMedChem 1, 689–693.
Jahn, N., Brantl, S., Strahl, H., 2015. Against the mainstream: the membrane-associated type I toxin BsrG from *Bacillus subtilis* interferes with cell envelope biosynthesis without increasing membrane permeability. Mol. Microbiol. 98, 651–666.
Kawai, Y., Daniel, R.A., Errington, J., 2009. Regulation of cell wall morphogenesis in *Bacillus subtilis* by recruitment of PBP1 to the MreB helix. Mol. Microbiol. 71, 1131–1144.
Kirstein, J., Hoffmann, A., Lilie, H., Schmidt, R., Rübsamen-Waigmann, H., Brötz-Oesterhelt, H., Mogk, A., Turgay, K., 2009a. The antibiotic ADEP reprogrammes ClpP, switching it from a regulated to an uncontrolled protease. EMBO Mol. Med. 1, 37–49.
Kirstein, J., Moliere, N., Dougan, D.A., Turgay, K., 2009b. Adapting the machine: adaptor proteins for Hsp100/Clp and AAA+ proteases. Nat. Rev. Microbiol. 7, 589–599.
Lee, B.G., Park, E.Y., Jeon, H., Sung, K.H., Paulsen, H., Rübsamen-Schaeff, H., Brötz-Oesterhelt, H., Song, H.K., 2010. Structures of ClpP in complex with a novel class of antibiotics reveal its activation mechanism. Nat. Struct. Mol. Biol. 17, 471–478.
Li, D.H., Chung, Y.S., Gloyd, M., Joseph, E., Ghirlando, R., Wright, G.D., Cheng, Y.Q., Maurizi, M.R., Guarne, A., Ortega, J., 2010. Acyldepsipeptide antibiotics induce the formation of a structured axial channel in ClpP: a model for the ClpX/ClpA-bound state of ClpP. Chem. Biol. 17, 959–969.
Malik, I.T., Brötz-Oesterhelt, H., 2017. Conformational control of the bacterial Clp protease by natural product antibiotics. Nat. Prod. Rep. 34, 815–831.
Monk, I.R., Shah, I.M., Xu, M., Tan, M.W., Foster, T.J., 2012. Transforming the untransformable: application of direct transformation to manipulate genetically *Staphylococcus aureus* and *Staphylococcus epidermidis*. mBio 3.
Morimoto, T., Loh, P.C., Hirai, T., Asai, K., Kobayashi, K., Moriya, S., Ogasawara, N., 2002. Six GTP-binding proteins of the Era/Obg family are essential for cell growth in *Bacillus subtilis*. Microbiology 148, 3539–3552.
Olivares, A.O., Baker, T.A., Sauer, R.T., 2016. Mechanistic insights into bacterial AAA+ proteases and protein-remodelling machines. Nat. Rev. Microbiol. 14, 33–44.
Pedelacq, J.D., Cabantous, S., Tran, T., Terwilliger, T.C., Waldo, G.S., 2006. Engineering and characterization of a superfolder green fluorescent protein. Nat. Biotechnol. 24, 79–88.
Peters, J.M., Colavin, A., Shi, H., Czarny, T.L., Larson, M.H., Wong, S., Hawkins, J.S., Lu, C.H.S., Koo, B.M., Marta, E., Shiver, A.L., Whitehead, E.H., Weissman, J.S., Brown, E.D., Qi, L.S., Huang, K.C., Gross, C.A., 2016. A comprehensive, CRISPR-based functional analysis of essential genes in bacteria. Cell 165, 1493–1506.
Pinho, M.G., Errington, J., 2003. Dispersed mode of *Staphylococcus aureus* cell wall synthesis in the absence of the division machinery. Mol. Microbiol. 50, 871–881.
Pinho, M.G., Errington, J., 2005. Recruitment of penicillin-binding protein PBP2 to the division site of *Staphylococcus aureus* is dependent on its transpeptidation substrates. Mol. Microbiol. 55, 799–807.
Popham, D.L., Setlow, P., 1996. Phenotypes of *Bacillus subtilis* mutants lacking multiple class A high-molecular-weight penicillin-binding proteins. J. Bacteriol. 178, 2079–2085.
Sambrook, J., Fritsch, E.F., Maniatis, T., 1989. Molecular Cloning. A Laboratory Manual, 2nd edition ed. Cold Spring Harbor, NY.
Sanchez-Gorostiaga, A., Palacios, P., Martinez-Arteaga, R., Sanchez, M., Casanova, M., Vicente, M., 2016. Life without division: Physiology of *Escherichia coli* FtsZ-deprived filaments. mBio 7.
Sass, P., Brötz-Oesterhelt, H., 2013. Bacterial cell division as a target for new antibiotics. Curr. Opin. Microbiol. 16, 522–530.
Sass, P., Josten, M., Famulla, K., Schiffer, G., Sahl, H.G., Hamoen, L., Brötz-Oesterhelt, H., 2011. Antibiotic acyldepsipeptides activate ClpP peptidase to degrade the cell division protein FtsZ. Proc. Natl. Acad. Sci. U. S. A. 108, 17474–17479.
Schindelin, J., Arganda-Carreras, I., Frise, E., Kaynig, V., Longair, M., Pietzsch, T., Preibisch, S., Rueden, C., Saalfeld, S., Schmid, B., Tinevez, J.Y., White, D.J., Hartenstein, V., Eliceiri, K., Tomancak, P., Cardona, A., 2012. Fiji: an open-source platform for biological-image analysis. Nat. Methods 9, 676–682.
Stokes, N.R., Baker, N., Bennett, J.M., Berry, J., Collins, I., Czaplewski, L.G., Logan, A., Macdonald, R., Macleod, L., Peasley, H., Mitchell, J.P., Nayal, N., Yadav, A., Srivastava, A., Haydon, D.J., 2013. An improved small-molecule inhibitor of FtsZ with superior in vitro potency, drug-like properties, and in vivo efficacy. Antimicrob. Agents Chemother. 57, 317–325.
Surdova, K., Gamba, P., Claessen, D., Siersma, T., Jonker, M.J., Errington, J., Hamoen, L.W., 2013. The conserved DNA-binding protein WhiA is involved in cell division in *Bacillus subtilis*. J. Bacteriol. 195, 5450–5460.
Wu, L.J., Errington, J., 2004. Coordination of cell division and chromosome segregation by a nucleoid occlusion protein in *Bacillus subtilis*. Cell 117, 915–925.
Wu, L.J., Ishikawa, S., Kawai, Y., Oshima, T., Ogasawara, N., Errington, J., 2009. Noc protein binds to specific DNA sequences to coordinate cell division with chromosome segregation. EMBO J. 28, 1940–1952.